Adaptation of Mode Filtering Technique in 4G-LTE Hybrid RoMMF-FSO for Last-mile Access Network

Hassan K. Al-Musawi, Tamas Cseh, Jan Bohata, Wai Pang Ng, Zabih Ghassemlooy, Stanislav Zvanovec, Eszter Udvary, and Petr Pesek

***Abstract*—This paper demonstrates a hybrid radio over multi-mode fibre and free space optics (RoMMF-FSO) system that can be used to extend the transmission range of the 4th generation long-term evolution (4G-LTE) signal in access networks. A single mode filtering technique (SMFT) is used to enhance 4G-LTE performance. The proposed scheme is evaluated in terms of the system transfer function, laser beam profile, and error vector magnitude (EVM). We show that using SMFT increases the RoMMF-FSO system bandwidth by 2 GHz and improves the received optical power by 13.6 dB. Moreover, the proposed system enhances the EVM by 4%. The measured results show that using a 1 km MMF instead of a 1 km SMF will marginally increase the measured EVM from ~6.6% to ~7% with a 0.2 dB power penalty with respect to the LTE EVM limit of 12.5% as is specified for 16-quadrature amplitude modulation. The proposed system is validated practically under atmospheric turbulence conditions to mimic the outdoor environment. Measured EVM results are verified theoretically through transmitting LTE signals with turbulent using log-normal model. We also show that for a FSO link span of 500 m to meet the EVM target of 12.5% the SNR power penalties are ~2 dB and ~11 dB for σ_R^2 of 1.2×10^{-4} and 0.1, respectively compared with no turbulence.**

***Index Terms*— Free space optics, long term evolution, multimode optical fibres, radio-over-fibre.**

I. Introduction

THE rapid increase of the mobile communications with the growing demand for higher data rate applications have led to the 4th generation-long term evolution (4G-LTE), which is currently adopted by the most mobile operators worldwide to enhance the mobile network capacity, coverage and access speeds. However, continuing growth of data traffic and the increasing number of end user have created challenges in meeting the quality of service (QoS) requirements. A survey by Ericson [1] has shown that the data traffic increased by 14% quarter-on-quarter and 65% year-on-year, and it is expected to grow with ten-fold by the end of 2021.

The radio-over-fibre (RoF) technology can improve the coverage by adopting enhanced NodeB (eNB) and home eNB (HeNB) for the access and in-building networks, respectively. Single-mode-fibre (SMF) is used traditionally for the long distance applications due to its low attenuation, whereas the multi-mode-fibre (MMF) is mostly used for short distance applications [2]. In [3] the coverage of eNB was extended up to 2.1 km using the RoF technology based on SMF. Commercial LTE-RoF solutions were demonstrated by CommScope for in-building applications using distributed antenna system to overcome high RF signal penetration losses [4]. Meanwhile, an experimental demonstration of transmitting LTE over 525 m MMF was reported in [5] at wavelength, λ of 1310 nm with a ~3% error vector magnitude (EVM). At present, MMFs, identified by their optical multi-mode (OM), have different modal bandwidth as outlined in the ISO/IEC 11801 standard [6], and are considered for use as a fibre backbone infrastructure in existing buildings. OM1-4 can support data rates up to 1 and 10 Gbps, respectively [5]. MMF types are defined under over-filled launch (OFL) bandwidth, which refers to a launching technique that uses a light source with a spot size larger than the fibre core diameter. The typical OFL bandwidth-distance products of OM1, OM2, OM3 and OM4 at 850 nm are 200, 500, 1500 and 3500 MHz·km, respectively [6]. A survey in [2] highlighted that ~17 million km of MMF are installed in-building networks worldwide. However, in such fibres the modal dispersion induced pulse broadening that limits the available bandwidth severely [2]. Accordingly, several techniques have been proposed to mitigate the impact of the number of co-propagating modal groups at the receiver (Rx) including the single mode filtering technique (SMFT) [7], and the offset launch technique [8].

In addition to RoF, there is the complementary technology of free space optics (FSO), which can be used in the "last mile" of the access networks in urban/rural areas to deliver RF type signals. This technology is referred to as radio-over-FSO (RoFSO), which offers high bandwidth, immunity to the electromagnetic interference, and free license fees compared to

Manuscript received XXX XX, 2016; One of the authors Hassan K. Al-Musawi has a PhD sponsorship from the Ministry of Higher Education and Scientific Research, Iraq, and he is with the University of Kufa, Najaf, Iraq. (e-mail: {hasank.baqir@uokufa.edu.iq). The work is also supported by the EU COST Action IC1101 (OPTICWISE).

The authors Hassan K. Al-Musawi, Wai Pang Ng, and Zabih Ghassemlooy are with Optical Communication Research Group, Northumbria University, Newcastle upon Tyne, NE1 8ST, UK. (e-mail: {hassan.al-musawi, wai-pang.ng, z.ghassemlooy}@northumbria.ac.uk).

Tamas Cseh and Eszter Udvary are with the Department of Broadband Information and Electromagnetic Theory, Budapest University of Technology and Economics (e-mail: {tcseh, eszter.udvary}@mht.bme.hu).

Jan Bohata, Stanislav Zvanovec and Petr Pesek are with the Department of Electromagnetic Field, Czech Technical University in Prague, Czech Republic, (e-mail: {bohatja2, xzvanove, pesekpe3}@fel.cvut.cz).

RF wireless communications. At present, commercial FSO products offer data rates up to 10 Gbps (e.g., TereScope 10GE produced by MRV [9]). Higher data rate of 1.6 Tbps using a single FSO link was reported experimentally in [10]. The link performance of FSO systems are affected by the atmospheric channel conditions such as atmospheric absorption, scattering, and scintillation, which affect the transmission quality as well as the link availability [11, 12]. Scintillation is a random phenomenon initiated by small temperature variations along the optical path, i.e., optical turbulence, thus leading to the refractive index and irradiance fluctuations [13]. In [14] several schemes have been introduced to combat turbulence induced fading effects. The impact of turbulence on the propagating optical beam can be evaluated using several statistical models including log-normal and gamma-gamma distribution model, which are adopted for weak and weak-strong turbulence regimes, respectively [12]. Here we have adopted log-normal model to experimentally assess the performance of proposed system under weak turbulence.

The combination of RoF and RoFSO can be used in both access and in-building networks to deliver higher data rates services. RoFSO can be used as a bridge between multi-RoF systems, where there is no fibre optic infrastructure in place particularly in rural areas. In [15] an analytic model for transmission of an orthogonal frequency division multiplexing (OFDM) signal over a FSO link was reported, showing that RoFSO is highly sensitive to the atmospheric turbulence, received optical power and modulation index. In [16], experimental investigation of the work in [15] was reported whereby a digital TV based RF signal was transmitted over a 1 km FSO link at λ of 1550 nm. Further research works have considered mainly the atmospheric effects on the FSO link when using short length SMFs, but not the perturbing effects generated by MMF. In [12] experimental demonstration of the baseband signal transmission at 100 Mbps over a 1 m of MMF and a 2.5 m of a FSO link with weak turbulence was reported with a packet error rate (PER) of ~10^{-2} using coding. Furthermore, an experimental RoF and RoFSO systems using the RF frequency range of 0.4 - 4 GHz and a 10 km of SMF were reported in [17].

In this paper, we propose a hybrid radio over MMF and FSO (RoMMF-FSO) system for the last metre (inter-room networks) and the last mile of the access networks as presented in Fig. 1. Line-of-sight FSO links can be used to inter-connect rooms and buildings with transmission spans up to a few kilometres. Indoor RoF systems with MMF are deployed for connecting the residential gateway (RG) with HeNB. We propose a mode filtering technique and carry out theoretical and experimental verifications to mitigate the modal effects with the aim of improving the system performance in terms of the channel transfer function, optical beam profile, and EVM for a range of signal-to-noise ratio (SNR). The remaining of the paper is organized as follows: Section II explains the theory of the proposed system. Section III demonstrates the experimental setup while the obtained results are presented and discussed in section IV. Finally, section V concludes the findings of the paper.

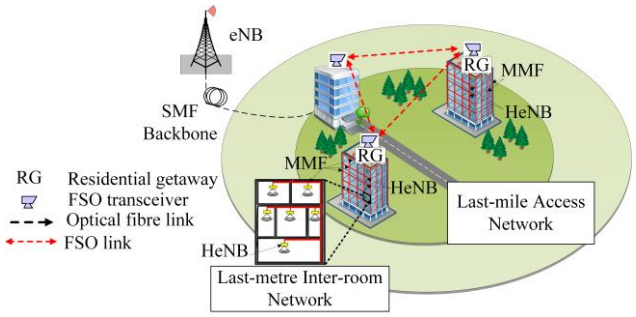

Fig.1: RoMMF-FSO scenario providing wireless services in the last-metre and last-mile access networks

II. THEORETICAL MODEL

The proposed system shown in Fig. 2 is modelled using MATLAB™ with the following principal aspects:

A. *Hybrid linear model*

The hybrid RoMMF-FSO link can be separated into three different sections, transmitter (Tx), Rx and optical channel, which includes the fibre to free space interface, see Fig. 2. At the Tx the OFDM LTE and baseband signals are generated with the latter composed of 16-quadrature amplitude modulation (16-QAM) at 20 MHz as a single-carrier modulation (SCM) $\boldsymbol{X}(m)$ where m=0, 1, …, N-1 is the subcarrier index, and N=128 is the number of subcarriers. An N–point inverse Fourier transform (IFFT) is applied to generate the OFDM signal $\boldsymbol{S}(n)$. The cyclic prefix (CP) is added at the rate of 1/4 to generate the OFDM signal with CP $\boldsymbol{S}_{\text{cp}}(n)$ to avoid inter-symbol interference (ISI), which is then passed through a parallel-to-serial converter (P/S) and a digital-to-analogue (DAC) converter. The continuous signal $\boldsymbol{S}_{\text{cp}}(t)$ is then converted into a passband OFDM signal $\boldsymbol{S}_{\text{RF}}(t)$ at 2.6 GHz, which is the most common LTE band deployed in Europe [18]. The LTE signal reported in [19] is used to externally modulate the output of a distributed feedback (DFB) laser using a Mach–Zehnder modulator (MZM). Details of the transmitted optical field at the output of MZM can be found in [19]. The output of MZM is amplified by an erbium-doped fibre amplifier (EDFA) to compensate for the link loss and ensure a sufficient link power budget prior to transmission over 1 km, 1 m and 2 m of MMF, SMF and FSO links, respectively. A patch cord SMF is used as a mode filter between SMF and FSO. At the Rx, following optical to electrical conversion using a photodetector (PD), the modulated signal is down converted to 20 MHz using a local oscillator running at the same frequency of 2.6 GHz as in the Tx. The remaining parts of the Rx is exactly the same as the Tx except for the frequency domain zero forcing equalizer (ZF), which is used to compensate for phase and amplitude distortions incurred by the propagating signal. In this work we have made a number of assumptions including: (*i*) a linear MZM (i.e., chirp-free); (*ii*) no fibre nonlinearities since the optical power level is relatively low not exceeding 10 dBm [20]; and (*iii*) a non-selective frequency FSO channel since the FSO link has a negligible delay spread [14]. Note that, the proposed link in a clear channel is time invariant, therefore, it can be modelled as a linear time-invariant system and can be defined in terms of

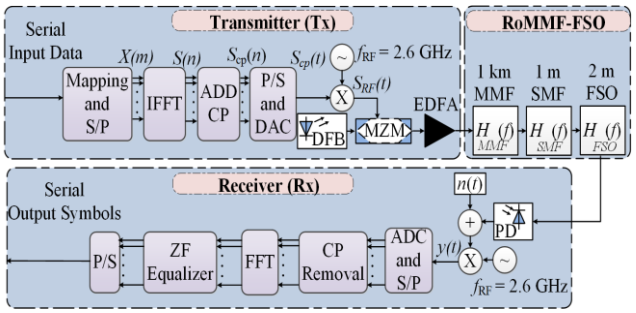

Fig. 2: Theoretical model of RoMMF-FSO system

the link transfer function, which depends strongly on the modal group delay and the modal power distribution determined by the link characteristics and launching conditions at the Tx/Rx ends and the intermediate MMF/SMF interface [21].

B. Fibre channel

The modulated optical signal is launched into the free space via MMF and SMF as depicted in Fig. 2. The total transfer function $H_{total}(f)$ is given as:

$$H_{total}(f) = H_{MMF}(f) \cdot H_{SMF}(f) \cdot H_{FSO}(f), \quad (1)$$

where $H_{MMF}(f)$, $H_{SMF}(f)$ and $H_{FSO}(f)$ are the transfer function for MMF, SMF and FSO channels, respectively. $H_{MMF}(f)$ is given as [22]:

$$H_{MMF}(f) = \overbrace{\exp\left[-\frac{(2\pi f D L \sigma_\lambda)^2}{2}\right]}^{\text{First term}} \cdot \overbrace{\sum_{k=1}^{K} P_k \exp(-j2\pi f \tau_k L) \cdot 10^{-\alpha_k L/10}}^{\text{Second term}}, \quad (2)$$

where f is the modulating frequency, D [ps/nm.km] is the chromatic dispersion coefficient, L is the fibre length [km], σ_λ is the root-mean-square value of the laser linewidth [nm], K is the total number of the mode groups, P_k, τ_k and α_k are the input power, group delay and mode dependent attenuation coefficient of the k^{th} mode group, respectively. Note that, the first and second terms in (2) represent the chromatic and modal dispersions, respectively. Chromatic dispersion depends on the spectral extent of the light source, while modal dispersion is due to different propagation velocity of the mode groups. For the refractive index with a parabolic profile in the fibre core, the total number of mode groups can be approximated by [23]:

$$K = \left(\pi d_{MMF} n_{eff} / \lambda\right)\left(g \cdot \Delta / g + 2\right)^{1/2}, \quad (3)$$

where d_{MMF} is the MMF core diameter, n_{eff} is the effective refractive index of the MMF core, g is the refractive index profile parameter and Δ is the refractive index contrast.

The linear $H_{SMF}(f)$ describes the chromatic dispersion effect in addition to the SMF attenuation. However, these effects can be neglected due to the short length of SMF (i.e., 1 m). However, the insertion loss due to coupling between MMF and SMF is considered in this work, see Table I. As shown in Fig. 2, to ensure propagation of the fundamental mode in the free space channel the output of MMF is applied to SMF, which acts as a mode filter. Accordingly, the transfer function of the filtered beam can be defined as:

$$H_{filtered}(f) = H_{MMF}(f) \cdot H_{SMF}(f), \quad (4)$$

which is approximated using (2) as:

$$H_{filtered}(f) = \exp\left[-\frac{(2\pi f D L \sigma_\lambda)^2}{2}\right] \cdot P_1 \exp(-j2\pi f \tau_1 L) \cdot 10^{-\alpha_1 L/10}, \quad (5)$$

where P_1, τ_1 and α_1 are the power, group delay and the attenuation of the transmitted fundamental mode, respectively.

C. FSO channel

For modelling a clear FSO channel the simplest plane wave model is adopted, where the electrical field distribution can be modelled as the superposition of far field distributions of each mode groups. The far field delay different mode groups in the same way, therefore, a clear FSO channel can be modelled as a summative attenuation. A FSO channel state h representing the optical intensity fluctuations due to the atmospheric loss, turbulence- and misalignment-induced fading is defined as [9]:

$$h = h_l \cdot h_s, \quad (6)$$

where h_l and h_s denote attenuations due to beam extinction arising from scattering, absorption and geometric spread and scintillation, respectively. Note that, we have assumed no misalignment induced losses. h_l is a deterministic parameter and therefore is considered as a constant scaling factor over a long time scale compared to the bit intervals of ~10^{-9} s [24], which is given by [9]:

$$h_l = \left[A \Big/ \pi\left(\frac{\theta}{2} d_i\right)^2\right] \exp\left(-\beta_l d_i\right), \quad (7)$$

where $A = \pi(a/2)^2$ is the Rx aperture area, a is the Rx aperture diameter, θ is the divergence angle, d_i is the FSO span, and β_l is the atmospheric attenuation coefficient, which is ~0.43 dB/km for a clear channel condition [9]. h_s is time-variant factors, exhibiting variations in the fading channel in the order of milliseconds, in which their stochastic behaviour is described by their respective distributions [25].

The turbulence (scintillation) is caused by random variations in the refractive index of the medium along the transmission path. The refractive index structure parameter C_n^2 [$m^{-2/3}$] is widely used to measure the strength of the refractive index fluctuations, which is defined in [11]. C_n^2 is very sensitive to the small-scale temperature variations described by the temperature structure constant, which can be obtained from the mean square temperature difference of two adjacent temperature points as outlined in [13]. Turbulence is classified as weak, moderate and strong depending on the strength of scintillation and is defined using Rytov variance σ_R^2. σ_R^2 is deduced based on the assumption that the laser beam propagates in a plane wave with homogeneous turbulence (i.e., C_n^2 is constant along the horizontal path), which is given as [26]:

$$\sigma_R^2 = 1.23 C_n^2 w^{7/6} d_i^{11/6}, \quad (8)$$

where $w = (2\pi/\lambda)$ is the optical wave number. Note that, $\sigma_R^2 < 1$, $\sigma_R^2 \sim 1$ and $\sigma_R^2 > 1$ correspond to weak, moderate and strong turbulence regimes, respectively [11]. For weak turbulence log-normal distribution model is widely used to describe the FSO channel statistically with the probability density function (PDF) of the irradiance fluctuation is given by

[24]:

$$f_{h_s}(h_s) = \frac{1}{\sqrt{2\pi\sigma_X^2}} \frac{1}{h_s} \exp\left\{ - \frac{\left(\ln(h_s) + \sigma_X^2/2\right)^2}{2\sigma_X^2} \right\}, \quad (9)$$

where σ_X^2 is ~$\sigma_R^2/4$ for the case of plane wave propagation [24].

The link total transfer function can be approximated by:

$$H_{total}(f) = \left| H_{filterred}(f) \right| \cdot 10^{-\alpha_{total} L_{total}}, \quad (10)$$

where α_{total} and L_{total} are the total system attenuation and total channel distance, respectively.

III. Experimental Model

The schematic block diagram of the experimental setup for the proposed system is shown in Fig. 3. All the key relevant system parameters are presented in Table I. At the Tx, the LTE signal (i.e., 16-QAM with a passband frequency of 2.6 GHz and at a bit rate of 67 Mbps) is generated using a Rohde&Schwarz (R&S) VSG, which is used to externally modulate a DFB laser at λ of 1550 nm using MZM. Note that, a polarization controller (PC) is used to control the polarization of the DFB laser. A low noise EDFA and a variable optical attenuator are used to optimize the transmitted optical power prior to being launched into a 1 km OM2 MMF. As for the channel, three setups are considered, see Fig. 3, which depicts various inter-building network configurations. In all three setups collimating optical lenses are used to launch light from fibre into a free space channel and capture light from the channel into a fibre. The output of the Tx (i.e., a downlink (DL) LTE signal) is transmitted via (*i*) setup A– composed of 1 km MMF, 50 cm long free space channel and 2 m MMF; (*ii*) setup B - 1 km MMF, 1 m SMF, 2 m FSO channel and 1 m SMF. Additionally, a 1 km SMF is used instead of a 1 km MMF and a 1 m SMF to validate the proposed technique; and (*iii*) setup C - 1 km MMF, 1 m SMF, 2 m FSO channel, 1 m SMF and 100 m MMF. Note that, a 100 m MMF represents the fibre length used in an indoor environment. In Setups B and C pigtailed GRIN lenses are used to align the optical beam propagating through the FSO channel. The GRIN lens can correct the monochromatic aberrations as well as enhance the alignment tolerance and the coupling efficiency (fibre to FSO and FSO to fibre) [27].

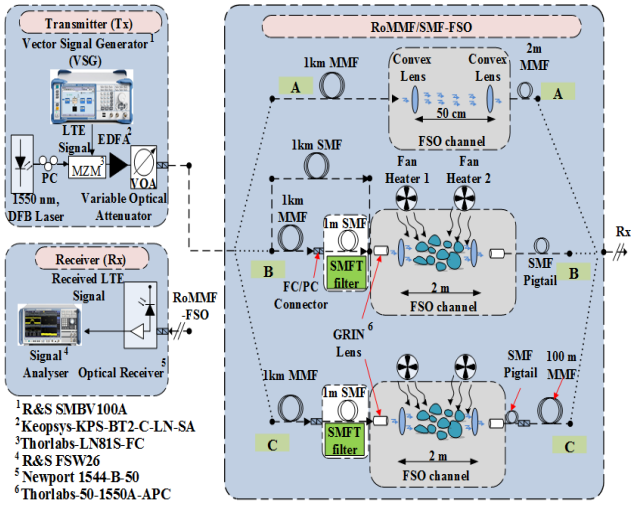

Fig. 3: Experimental setup of RoMMF-FSO system with three scenarios

TABLE I: SYSTEM PARAMETERS

Parameter	Values
Modulation scheme	16-QAM
Baseband multiplexing	OFDM
Carrier frequency	2.6 GHz
Signal bandwidth, bit rate	20 MHz, 67 Mbps
RF power	-10 dBm
DFB wavelength, power	1550 nm, 6 dBm
Relative intensity noise (RIN)	-145 dB/Hz
MZM insertion loss	6 dB
EDFA gain, noise figure	13.5 dB, 3 dB
MMF d_{MMF}, n_{eff}, α_1, Δ	50 µm, 1.45, 0.3 dB/km, 0.01
SMF loss @ 1550 nm	0.15 dB/km
MMF/SMF coupling loss	1.7 dB
FSO total loss	15 dB
GRIN lens aperture	1.8 mm
Plano-convex lens diameter	25.4 mm
PIN PD responsivity	0.75 A/W
TIA 3dB bandwidth	DC to 12 GHz

At the Rx, a combination of PIN PD and a trans-impedance amplifier (TIA) are used to regenerated the electrical LTE signal, which is captured using a real-time signal analyser for off-line signal processing including equalization [28], demodulation and link performance assessment. In order to validate the proposed system performance under atmospheric turbulence we have used a dedicated indoor FSO chamber to mimic the outdoor environment. To generate turbulence two fans were used to blow hot and cold air into the chamber perpendicularly to the propagating optical beam. Twenty temperature sensors with a spacing of 10 cm were deployed along the chamber to monitor and measure the temperature profile. In order to create different scintillation effects, two levels of thermal gradient of 6° C and 31° C were introduced to the chamber. These values are then used to determine the turbulence strength in terms of C_n^2 and then σ_R^2 using (8). For weak turbulence calculated values of C_n^2 are 5.37×10^{-13} and 4.09×10^{-10} $m^{-2/3}$ and for d_i = 2 m the values of σ_R^2 are 1.2×10^{-4} and 0.1, respectively.

IV. Results and Discussions

In this section, we evaluate the performance of SMFT in terms of the measured system transfer function and the laser beam profile. Moreover, the influence of atmospheric turbulence on LTE signals transmitted over RoMMF-FSO links is investigated theoretically and practically. The measured system performance is validated in terms of the EVM by using MATLAB™ simulations.

A. Transfer function

The transfer function of the overall system is measured using the Agilent E5071C ENA network analyser. The system transfer function describes perturbing effects on the propagating optical beams along MMF and FSO channels due to the multi-mode propagation within MMF as described in (2). Fig. 4 shows transfer function of the RoMMF-FSO system for setups A, B and C. At low frequencies, the transfer function for the setup A with no SMFT shows degrading in the system gain

due to high attenuation and dispersion with a maximum drop at 1 GHz. It turned out that the system performance fluctuates beyond the baseband showing highly sensitive performance to frequency changes. Furthermore, it shows a limited passband bandwidth to ~1 GHz (by considering ~1.45 GHz and ~2.45 GHz as the lower and upper cut-off frequencies, respectively). This means that the LTE based OFDM signal at a 2.6 GHz carrier frequency will experience frequency selective fading, thus resulting in corrupted orthogonality that leads to the channel induced ISI [29]. On the contrary, the transfer functions for the setups B and C depict a significant enhancement in the frequency dependent stability when SMFT is adopted compared to the Setup A. The SMFT interface can filter out higher order modes, thus making the system transfer function much flatter by minimizing the number of modal groups as is evident by a significant reduction in the ripple level from ~5 dB to < 1 dB and hence enhancing the channel bandwidth effectively for a wider range up to 3 GHz. Furthermore, Fig. 4 compares experimental results with predicted $H_{total}(f)$ of the MMF-FSO system (10). The difference between them at low frequencies (f < 1 GHz) is due to no consideration of the transfer function of the optoelectronic devices (i.e., MZM and PD) in the theoretical model.

B. *Optical beam profile*

The beam profile was captured in real-time using a BP104-IR beam scanning profiler from Thorlabs. Fig. 5 illustrates the measured laser beam profiles for the setups A and B for two different turbulence strengths (i.e., σ_R^2) in addition to the clear FSO channel. Furthermore, Table II presents a summary of the obtained results. The beam profile shows the optical power distribution at a plane transverse to the beam propagation path. Fig. 5(a) shows the peak power of the received beam for the two setups. For the setup A with no filtering the received signal is attenuated severely due to several reasons such as the lack of alignment, a large divergence angle, and modal effects. In contrast, using SMFT (setup B) can overcome these effects significantly. Table II illustrates the enhancement of the peak received optical power showing significant improvement in the coupling efficiency, which determined with respect to setup A. Fig. 5(b) displays the normalized power of the beam profile to illustrate beam width in terms of the full width at half maximum (FWHM). The optical beam is subjected to the shape deformations, which is mainly due to the diffraction and deflection that can cause a variation in the power levels of the received signal. For the received beam in setup A, the measured beam profile has several peaks and the beam profile is relatively

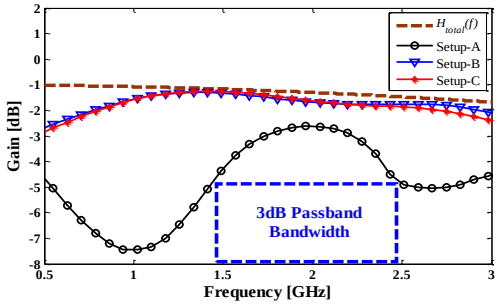

Fig. 4: Transfer function of the RoMMF-FSO system

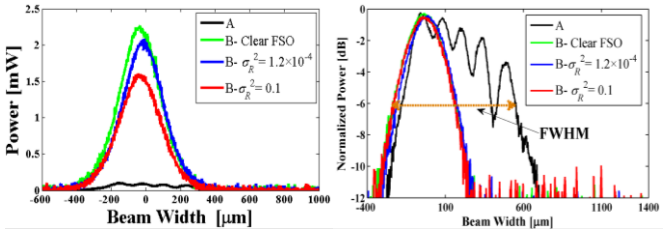

(a) (b)

Fig. 5: Beam profile of the RoMMF-FSO system shown turbulence effect on: (a) Amplitude, and (b) FWHM

wide. Even though MMF can support propagation of a large number of modes, a finite number of modes clustered in groups with nearly the same propagation characteristics are considered [23]. For the fibre with the parabolic refractive index profile (i.e., g=2) the number of propagating mode groups K estimated using (3) is 10. A three-dimension (3D) illustration of the beam profile is depicted in Fig. 6. The beam distribution at the Rx, which is distorted while propagating along the channel with no SMFT, is shown in Fig. 6(a), whereas Fig. 6(b) illustrates the Gaussian distribution of the received optical beam following SMFT, which has eliminated high order modes.

C. *EVM results*

The EVM parameter demonstrates the impact of distortion induced in the system. The proposed system is designed to achieve < 12.5% EVM as a figure of merit required by the 3rd Generation Partnership Project (3GPP) LTE for 16-QAM modulation [30]. In the simulation model, the LTE signal was used to modulate the DFB laser externally using MZM. The MMF/SMF interface is modelled using (10), while the log-normal distribution model is used to simulate the FSO channel under the weak turbulence regime. Predicted EVM results are determined using (2) in [31] while the measured values are captured using the signal analyser that has built-in vector signal analyser (VSA) software. Firstly, we investigate the influence of SMFT with no turbulence induced the fading effect. Fig. 7 shows the measured EVM against the SNR for the three setups compared with the back-to-back (B2B) setup. In the setup A, the EVM values are high and not stable due to the irradiance fluctuation caused by the modal effects. On the other hand, it can be seen that the system performance is enhanced by using SMFT in setups B and C. At a SNR of 20 dB, EVM is reduced from ~11% to ~7% (i.e., 4% enhancement) when using a filter, which is identified as the setup B-MMF in Fig. 7. Additionally, a 1 km SMF was used in the setup B instead of a 1 km MMF and a 1 m SMF to validate the obtained results. The EVM value is decreased from ~7% to ~6.6% (i.e., 0.4% difference only) for the same SNR value (i.e., 20 dB) compared to a 1 km MMF. The EVM values were measured via the VSA with a precision of ±0.2% [28]. Note that, the EVM results are based on the average of three sets of measurements under identical

TABLE II: Beam profile characteristics

Setup	Peak Power (mW)	Coupling Efficiency (dB)	FWHM (μm)
A	0.1	--	374
B- clear FSO	2.3	13.6	258
B- σ_R^2=1.2×10^{-4}	2.1	13.22	267
B- σ_R^2=0.1	1.6	12	281

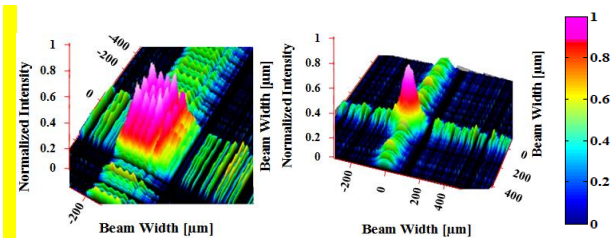

(a) (b)

Fig. 6: 3D illustration of the beam profile: (a) with no SMFT, and (b) with SMFT.

conditions. The additional power of the input signal required to achieve the EVM limit is referred to the power penalty (PP). PPs with respect to the B2B link are 3.9 dB, 0.5 dB, 0.3 dB and 2.3 dB for the setups A, B-MMF, B-SMF and C, respectively. The PP difference between the setup-B-SMF and the setup-B-MMF is 0.2 dB. The turbulence effect is investigated theoretically and practically using the setups B and C in terms of EVM measurements as illustrated in Figs. 8 and 9, respectively. The inset figures show the measured constellation diagrams for the received LTE signal with turbulence i.e., σ_R^2 of 0.1. Note that, all constellation diagrams in this paper have been captured for the SNR of 20 dB. Fig. 8 depicts predicted and measured EVM values for the two levels of turbulence strength for the FSO channel as in the setup B. The simulation results show a good agreement compared to the measured SNR values at the EVM limit with < 1 dB difference at σ_R^2 of 0.1. The summary of the measured EVM and PPs are presented in Table III for a clear FSO channel and two turbulence strengths. The results show that for increased turbulence strength the EVM levels are deteriorated due to the optical intensity fluctuations and fading caused by the random variation of the air refractive index. Note that, the turbulence strength (i.e., σ_R^2) depends on the temperature gradient along the propagation channel [26]. Consequently, a further spreading of the PDF of the received signal can be induced as a result of signal fading [13]. The PPs with respect to a clear channel shown in Table III indicates that at higher turbulence level (i.e., σ_R^2 of 0.1 experienced in case of C_n^2 of 4.09×10^{-10} $m^{-2/3}$) the PP is increased by ~2 dB. In order to compare the setups B and C, we have kept turbulence levels the same. Fig. 9 depicts the predicted and measured EVM values for the setup C, while the obtained results are outlined in Table III, which shows an increase in the required SNR values to achieve the EVM limit due to the additive loss and dispersion. In addition, the end-to-

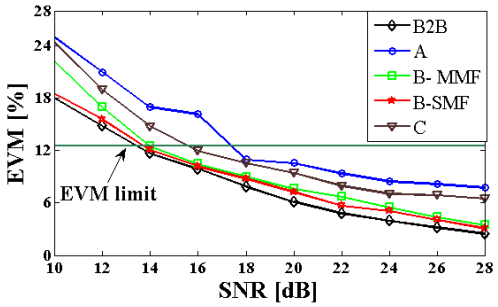

Fig. 7: Measured EVM performance of the RoMMF-FSO system

end simulation shows the same trend for measured SNR values. However, the measured SNR values show an increase by ~ 2 dB at the EVM limit for σ_R^2 of 0.1 compared to the simulation due to the intensity fluctuations of ±0.3% of the experimental EVM measurements. This intensity fluctuation is magnified by the modal effects generated by the additional MMF following the FSO. Furthermore, the EDFA amplified spontaneous noise (ASE) does affect the system performance, which is not considered in this work and will be studied in the future.

Finally, we carried out further analyses for the FSO path of 500 m long, which is the typical range for the last-mile access network in the urban areas [32]. Fig. 10 illustrates the predicted EVM as a function of SNR with weak turbulence (i.e., σ_R^2 = 1.2×10^{-4} and 0.1) and no turbulence. The results show that in order to achieve the 3GPP LTE EVM target of 12.5% the SNR power penalties are ~2 dB and ~11 dB for σ_R^2 of 1.2×10^{-4} and 0.1, respectively compared with no turbulence case.

V. Conclusions

In this paper, the hybrid RoMMF-FSO scheme was demonstrated to enhance the performance of the 4G-LTE signal for radio over indoor MMF system as part of the last mile access networks. We showed that adopting SMFT can reduce the EVM level, in addition to mitigating the modal effects within the MMF-FSO interface did results in a negligible difference compared to SMF-FSO in terms of EVM and PPs. Moreover, the proposed system improved the available channel bandwidth by 2 GHz at least due to reduced level of ripple fluctuation in the system transfer function by 4 dB. Additionally, the laser beam profile measurements showed that the use of SMFT can enhance the received power and FWHM significantly. We also experimentally and theoretically validated the performance of the proposed system under turbulence by transmitting the LTE

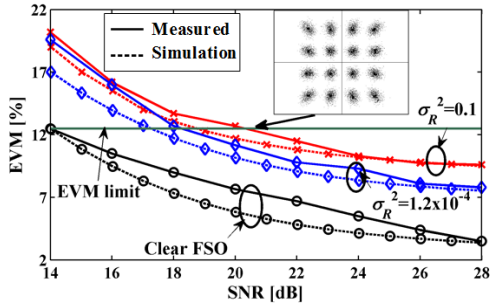

Fig. 8: Measured and theoretical EVM performance of the setup B under clear air condition and two weak turbulence levels

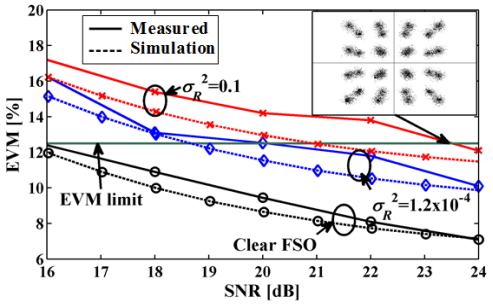

Fig. 9: Measured and theoretical EVM performance of the setup C under clear air condition and two weak turbulence levels

TABLE III: Measured SNR and PP at EVM limit for the setups B and C

	Setup B		Setup C	
Turbulence Strength	**SNR (dB)**	**PP (dB)**	**SNR (dB)**	**PP (dB)**
Clear FSO	14.1	--	15.8	--
σ_R^2=1.2×10^{-4}	18.25	4.15	20	4.2
σ_R^2=0.1	20.33	6.23	23.55	7.75

signal over the MMF and FSO channels. We also showed that for the FSO link span of 500 m to meet the EVM target of 12.5% the SNR power penalties were ~2 dB and ~11 dB for σ_R^2 of 1.2×10^{-4} and 0.1, respectively compared with no turbulence.

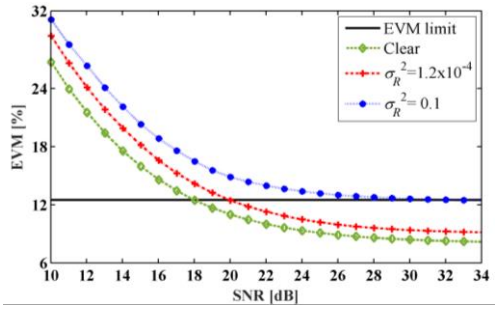

Fig. 10: Analysed EVM performance for FSO span of 500 m

REFERENCES

[1] S. Carson and P. Jonsson, "Ericsson mobility report: On the pulse of the networked society ", Stockholm, November 2015.

[2] G. S. D. Gordon, M. J. Crisp, R. V. Penty, T. D. Wilkinson, and I. H. White, "Feasibility demonstration of a mode-division multiplexed MIMO-enabled radio-over-fiber distributed antenna system," *J. of Lightwave Tech*, vol. 32, pp. 3521-3528, 2014.

[3] A. Nagate, K. Hoshino, M. Mikami, and T. Fujii, "A field trial of multi-cell cooperative transmission over LTE system," in *2011 IEEE Intern. Conf. on Communications (ICC)*, 2011, pp. 1-5.

[4] CommScope, "In-Building Wireless Solutions," 2012.

[5] D. Visani, M. N. Petersen, F. Sorci, L. Tarlazzi, P. Faccin, and G. Tartarini, "In-building wireless distribution in legacy multimode fiber with an improved RoMMF system," *Microwave and Wireless Components Letters, IEEE*, vol. 22, pp. 598-600, 2012.

[6] R. E. Freund, C. Bunge, N. N. Ledentsov, D. Molin, and C. Caspar, "High-speed transmission in multimode fibers," *J. of Lightwave Tech*, vol. 28, pp. 569-586, 2010.

[7] T. Cseh and T. Berceli, "Dispersion compensation in millimeter wave radio over fiber systems," *Microwave and Optical Tech. Letters*, vol. 57, pp. 204-207, 2015.

[8] K. Appaiah, R. Salas, S. Vishwanath, and S. R. Bank, "Offset coupling, feedback, and spatial multiplexing in 4,x,4 incoherent-MIMO multimode fiber links," *J. of Lightwave Tech*, vol. 31, pp. 2926-2939, 2013.

[9] P. V. Trinh, N. T. Dang, and A. T. Pham, "All-optical relaying FSO systems using EDFA combined with optical hard-limiter over atmospheric turbulence channels," *J. of Lightwave Tech*, vol. 33, pp. 4132-4144, 2015.

[10] G. Parca, A. Shahpari, V. Carrozzo, G. M. T. Beleffi, and A. L. Teixeira, "Optical wireless transmission at 1.6-Tbit/s (16× 100 Gbit/s) for next-generation convergent urban infrastructures," *Optical Engineering*, vol. 52, pp. 116102-116102, 2013.

[11] L. C. Andrews and R. L. Phillips, *Laser beam propagation through random media*, 2nd ed. Bellingham, Wash.: SPIE Press, 2005.

[12] R. Pernice, A. Parisi, A. And, xf, S. Mangione, G. Garbo, *et al.*, "Error mitigation using RaptorQ codes in an experimental indoor free space optical link under the influence of turbulence," *Iet Communications*, vol. 9, pp. 1800-1806, 2015.

[13] Z. Ghassemlooy, H. Le Minh, S. Rajbhandari, J. Perez, and M. Ijaz, "Performance analysis of ethernet/fast-ethernet free space optical communications in a controlled weak turbulence condition," *J. of Lightwave Tech*, vol. 30, pp. 2188-2194, Jul 1 2012.

[14] M. A. Khalighi and M. Uysal, "Survey on free space optical communication: A communication theory perspective," *IEEE Communications Surveys & Tutorials*, vol. 16, pp. 2231-2258, 2014.

[15] A. Bekkali, C. B. Naila, K. Kazaura, K. Wakamori, and M. Matsumoto, "Transmission analysis of OFDM-based wireless services over turbulent radio-on-FSO links modeled by gamma-gamma distribution," *IEEE Photonics Journal*, vol. 2, pp. 510-520, 2010.

[16] C. B. Naila, K. Wakamori, M. Matsumoto, A. Bekkali, and K. Tsukamoto, "Transmission analysis of digital TV signals over a radio-on-FSO channel," *IEEE Comm. Mag.*, vol. 50, pp. 137-144, 2012.

[17] J. Bohata, S. Zvanovec, M. M. Abadi, and Z. Ghassemlooy, "Channel characterization of a last-mile access radio over combined fibre and free-space optics system," in *2015 Intern. Conf. on Automation, Cognitive Science, Optics, Micro Electro-Mechanical System, and Info Tech (ICACOMIT)*, 2015, pp. 27-30.

[18] 3GPP, "Evolved universal terrestrial radio access (E-UTRA);physical channels and modulation," vol. 3GPP TS36.211 V10.4.0, Rel-10, 2011.

[19] T. Kanesan, W. P. Ng, Z. Ghassemlooy, and C. Lu, "Investigation of optical modulators in optimized nonlinear compensated LTE RoF system," *J. of Lightwave Tech*, vol. 32, pp. 1944-1950, 2014.

[20] G. P. Agrawal, *Nonlinear Fiber Optics*: Academic Press, 2013.

[21] M. G. Larrode and A. M. J. Koonen, "Theoretical and experimental demonstration of OFM robustness against modal dispersion impairments in radio over multimode fiber links," *J. of Lightwave Tech*, vol. 26, pp. 1722-1728, 2008.

[22] J. Siuzdak and M. Kowalczyk, "3x3 incoherent MIMO transmission over MM fiber," in *2011 2nd Intern. Conf. on Photonics*, 2011, pp. 1-4.

[23] G. Yabre, "Theoretical investigation on the dispersion of graded-index polymer optical fibers," *J. of Lightwave Tech*, vol. 18, pp. 869-877, 2000.

[24] A. A. Farid and S. Hranilovic, "Outage capacity optimization for free-space optical links with pointing errors," *J. of Lightwave Tech*, vol. 25, pp. 1702-1710, 2007.

[25] I. E. Lee, Z. Ghassemlooy, W. P. Ng, and M.-A. Khalighi, "Joint optimization of a partially coherent Gaussian beam for free-space optical communication over turbulent channels with pointing errors," *Optics Letters*, vol. 38, pp. 350-352, 2013.

[26] H. K. Al-Musawi, T. Cseh, J. Bohata, P. Pesek, W. P. Ng, Z. Ghassemlooy, *et al.*, "Fundamental investigation of extending 4G-LTE signal over MMF/SMF-FSO under controlled turbulence conditions," in *Communication Systems, Networks and Digital Signal Processing (CSNDSP), 2016 10th Intern. Symp. on*, 2016, pp. 1-6.

[27] J. Nagar, S. D. Campbell, and D. H. Werner, "Multi-objective optimization for GRIN lens design," in *Antennas and Propagation & USNC/URSI National Radio Science Meeting, 2015 IEEE Intern. Symp. on*, 2015, pp. 1326-1327.

[28] Rohde&Schwarz, "R&S FSW-K70 vector signal analysis user manual," ed. Munchen, Germany, 2015.

[29] S. Y. Sun, Y. L. Hu, H. H. Chen, and W. X. Meng, "Joint pre-equalization and adaptive combining for CC-CDMA systems over asynchronous frequency-selective fading channels," *IEEE Transactions on Vehicular Tech.*, vol. 65, pp. 5175-5184, 2016.

[30] 3GPP, "LTE; Evolved universal terrestrial radio access (E-UTRA); Base station (BS) radio transmission and reception (3GPP TS 36.104 Release 12)," vol. 12.6.0, 2015.

[31] H. K. Al-Musawi, W. P. Ng, Z. Ghassemlooy, C. Lu, and N. Lalam, "Experimental analysis of EVM and BER for indoor radio-over-fibre networks using polymer optical fibre," in *Networks and Optical Communications, 2015 20th European Conf. on*, 2015, pp. 1-6.

[32] N. A. M. Nor, Z, J. Bohata, P. Saxena, M. Komanec, S. Zvanovec, *et al.*, "Experimental investigation of all-optical relay-assisted 10 Gb/s FSO link over the atmospheric turbulence channel," *J. of Lightwave Tech*, vol. 35, pp. 45-53, 2017.